Free Radical Research, August 2013; 47(8): 614–623

ISSN 1071-5762 print/ISSN 1029-2470 online
DOI: 10.3109/10715762.2013.806797

informa
healthcare

ORIGINAL ARTICLE

Mitochondrial susceptibility in a model of paraquat neurotoxicity

A. Czerniczyniec, S. Lores-Arnaiz & J. Bustamante

Instituto de Bioquímica y Medicina Molecular (UBA-CONICET), Facultad de Farmacia y Bioquímica, Universidad de Buenos Aires, Buenos Aires, Argentina

Abstract

Paraquat is a highly toxic herbicide capable of generating oxidative stress and producing brain damage after chronic exposure. The aim of this research was to investigate the contribution of mitochondria to the molecular mechanism of apoptosis in an *in vivo* experimental model of paraquat neurotoxicity. Sprague-Dawley adult female rats received paraquat (10 mg/kg i.p.) or saline once a week during a month. Paraquat treatment increased cortical and striatal superoxide anion levels by 45% and 18%, respectively. As a consequence, mitochondrial aconitase activity was significantly inhibited in cerebral cortex and striatum. Paraquat treatment increased cortical and striatal lipid peroxidation levels by 16% and 28%, respectively, as compared with control mitochondria Also, cortical and striatal cardiolipin levels were decreased by 13% and 49%, respectively. Increased Bax and Bak association to mitochondrial membranes was observed after paraquat treatment in cerebral cortex and striatum. Also, paraquat induced cytochrome *c* and AIF release from mitochondria.

These findings support the conclusion that a weekly dose of paraquat during four weeks induces oxidative damage that activates mitochondrial pathways associated with molecular mechanisms of cell death. The release of apoptogenic proteins from mitochondria to cytosol after paraquat treatment would be the consequence of an alteration in mitochondrial membrane permeability due to the presence of high superoxide anion levels. Also, our results suggest that under chronic exposure, striatal mitochondria were more sensitive to paraquat oxidative damage than cortical mitochondria. Even in the presence of a high oxidative stress in striatum, equal levels of apoptosis were attained in both brain areas.

Keywords: superoxide anion, aconitase activity, cardiolipin peroxidation, apoptogenic proteins

Introduction

Paraquat (1,1′-dimethyl-4,4′-bipyridinium dichloride) is a highly toxic herbicide which is able to induce dopaminergic neuronal death. Extensive evidence indicates that *in vivo* paraquat treatment produces weak or moderate decrease in the number of dopaminergic neurons in the substantia nigra, striatal levels of dopamine, expression and activity of tyrosine hydroxylase and decrease in the inmunoreactivity of dopamine transporter [1–4]. However, the molecular mechanisms by which paraquat kills dopaminergic neurons are still poorly understood. Although paraquat toxicity mainly causes dopaminergic cell death in the substantia nigra, the presence of paraquat has been observed in striatum, hippocampus, frontal cortex, and cerebellum after repeated administration of this drug (10 mg/kg) to mice [5]. It is not clear which is the cause of the different vulnerability of other brain regions such as frontal cortex, primarily responsible for cognitive and motor responses or hippocampus, primarily responsible for learning, cognition and memory to paraquat-induced neurotoxicity [6–8]. Also, it is already known that paraquat-mediated neurotoxicity is gender specific, as males are more susceptible than females. In experimental models, systemic paraquat treatment (10 mg/kg) of male mice and rats reproduces Parkinson's Disease-like features, but the same model of treatment in female mice did not produce significant reductions of nigrostriatal dopamine, striatal TH fiber density, and motor impairments [9]. For this reason, experimental models of paraquat neurotoxicity in female rats could contribute to studying the premotor stages of Parkinson's disease.

Mitochondria are essential for survival. Their primary function is to support aerobic respiration and to provide energy for intracellular metabolic pathways. Also, they play a central role during the induction of apoptosis, leading to the organized degradation of cellular structure. It is postulated that alterations in mitochondrial function and in active oxygen species generation could play a role in the induction of different signaling pathways leading to neuronal death [10,11]. Several reports described that paraquat interacts with mitochondrial Complex I to generate superoxide anion and hydrogen peroxide (H_2O_2) [12–14]. We recently reported that a weekly dose of paraquat (10 mg/kg i.p.) during four weeks induced cortical and striatal mitochondrial dysfunction as shown by decreased in mitochondrial respiratory control, decreased Complex I activity, increased H_2O_2 production and loss of mitochondrial membrane potential [15]. The cytotoxic actions of paraquat clearly involve reactive oxygen species

Correspondence: Dr. Analía Czerniczyniec, Instituto de Bioquímica y Medicina Molecular, Facultad de Farmacia y Bioquímica, Universidad de Buenos Aires, Junín 956, C1113AAD, Buenos Aires, Argentina. Tel/Fax: +(5411) 4508-3646. E-mail: aczerni@ffyb.uba.ar

(Received date: 21 December 2012; Accepted date: 15 May 2013; Published Online: 14 June 2013)

overproduction, but its specificity for dopaminergic neurons and the possible involvement of intrinsic cell death pathways are still unclear. It is probably that protein and lipid oxidation could be related to these pathways due to the high oxidative stress reached after paraquat treatment.

Due to the fact that paraquat treatment induced mitochondrial dysfunction in cerebral cortex and striatum but not in hippocampus [15], the present study was undertaken to investigate the contribution of mitochondria to the molecular mechanism of apoptosis and elucidate the susceptibility of the different brain areas in an experimental model of paraquat-induced neurotoxicity in female rats. This study provides new data about mitochondrial dysfunction and apoptosis in the premotor stages of Parkinson's disease. Superoxide anion production, lipid peroxidation, cardiolipin content, aconitase, and superoxide dismutase activity, Bax, Bak, and Bcl-xl expression were examined in control and paraquat-treated animals. The release of cytochrome *c* and apoptosis-inducing factor (AIF) was also evaluated.

Methods

Animals

A total of 24 Sprague Dawley female rats (all acquired from School of Pharmacy and Biochemistry) weighing 200–250 g at the beginning of experiments (ca. 2.5 months old) were kept in a soundproof room under a 12:12 h light/dark cycle photoperiod (lights on at 07:00 hr) and controlled temperature (22 ± 2°C). Food and water were available *ad libitum.* Measures were taken to minimize the number of animals used and their pain and discomfort, according to the principles and directives of the European Communities Council Directives (86/609/EEC) and according to the NIH Guide for the Care and Use of Laboratory Animals. They also received approval from the local ethical committee. Paraquat was dissolved in saline and administered at a dose of 10 mg/kg i.p. Rats treated with paraquat ($n = 12$) received one injection weekly during 4 weeks (total doses = 4). Paraquat dose was chosen in accordance with earlier works [1,16]. Control animals ($n = 12$) were treated with saline i.p. once a week. Animals were sacrificed two days after the end of treatment.

Isolation of mitochondria

Brains were quickly removed. Dissection was performed as described by Madison and Edison with some modifications [17]. Immediately after dissection, cerebral cortex and striatum from three control or paraquat-treated rats were pooled for each experimental group. Tissues were weighed and homogenized (1:5 w/v) in an ice-cold medium consisting of 0.23 M mannitol, 0.07 M sucrose, 5 mM Hepes, and 1 mM EDTA, pH 7.4 (MSHE buffer). A protease inhibitor cocktail (1 μg/ml pepstatin, 1 μg/ml leupeptin, 0.4 mM PMSF, and 1 μg/ml aprotinin) was added to the homogenates and they were centrifuged at 700 *g* for 10 min to discard nuclei and cell debris. Then, the supernatant obtained was centrifuged at 8000 *g* for 10 min. The resulting pellet containing mitochondria was washed and resuspended in MSH buffer (0.23 M mannitol, 0.07 M sucrose, and 5 mM Hepes, pH 7.4) at a protein concentration of 20–25 mg/ml [15]. All procedures were carried out at 0–2°C. Mitochondrial samples were less than 2–4% contaminated with cytosolic components according to the amount of lactate dehydrogenase present in the samples.

Protein content was assayed by using Folin phenol reagent and bovine serum albumin as standard [18].

Flow cytometry studies

Flow cytometry assays were performed in a FACScalibur (Becton-Dickinson) equipped with a 488 nm argon laser and a 615 nm red diode laser.

Population with high FSC and SSC characteristics was chosen according to the typical mitochondrial size (3–5 μm) calibrated using Beads Calibrite (6 μm) (Becton Dickinson) for all the cytometric studies.

Determination of mitochondrial superoxide anion levels by MitoSOX fluorescence

Superoxide anion was detected using the fluorescent dye MitoSOX ($C_{43}H_{34}N_3IP$), a membrane-permeant and rapidly targeted mitochondrial superoxide indicator with excitation/emission maxima of 510/580 nm. We developed a special protocol by flow cytometry in order to detect the superoxide anion that is not dismutated by the Mn-SOD in isolated mitochondria. Equal protein concentration (mg protein/ml) was used in order to normalize the results: control cerebral cortex (0.106 ± 0.006), paraquat cerebral cortex (0.111 ± 0.004), control striatum (0.122 ± 0.006), and paraquat striatum (0.110 ± 0.007). Isolated cortical and striatal mitochondrial samples from control and paraquat-treated animals were loaded with 2.5 μM MitoSOX during 20 min at 37°C in MSH buffer supplemented with 5 mM malate, 5 mM glutamate, and 1 mM phosphate. The procedure was carried out in a dark room. Then mitochondria were acquired by a cytometer [19]. Autofluorescence was also evaluated in samples without probe. Antimycin A (0.5 μM), an inhibitor of the ubiquinone–cytochrome *c* reductase, was used as a positive control. A common marker (M1), indicating high relative fluorescence intensity (r.f.i.) of the mitochondrial population was used to quantify the superoxide anion levels in each experiment.

Evaluation of cardiolipin content

The positively charged probe acridine orange 10-nonyl bromide (nonyl acridine orange, NAO, λ_{em} 525 nm) binds specifically to the negatively charged cardiolipin molecule providing a direct and reliable method for evaluating the cardiolipin content in mitochondria [20–22]. Nomura et al. [23] reported that NAO associated selectively with cardiolipin monolayers but not to other kinds of

phospholipids. Also, they described that the binding of NAO to cardiolipin was decreased by autoxidation. NAO is not able to bind peroxidated cardiolipin (CL-OOH) producing a decreased NAO fluorescence [23]. Isolated cortical and striatal mitochondria respiring in a metabolic state 4 were loaded with 100 nM NAO during 20 min at 37°C in MSH buffer supplemented with 5 mM malate, 5 mM glutamate, and 1 mM phosphate and acquired by the cytometer as previously described. Antimycin A (0.5 μM), an inhibitor of the ubiquinone-cytochrome *c* reductase, and samples without probe were used as positive and negative controls, respectively. Events with high NAO fluorescence were quantified using a marker (M1), as level of mitochondrial cardiolipin content.

In order to normalize the results, equal mitochondrial protein concentrations were used in this experiment: cerebral cortex (control: 0.122 ± 0.005 mg/ml; paraquat: 0.128 ± 0.006 mg/ml) and striatum (control: 0.117 ± 0.006 mg/ml; paraquat: 0.122 ± 0.007 mg/ml).

Thiobarbituric acid-reactive substances production

The amount of thiobarbituric acid-reactive substances (TBARS) was determined by a fluorescence assay as described by Esterbauer et al. with some modifications [24]. Fresh isolated mitochondria were washed with 50 mM phosphate buffer (pH 7.4) in order to eliminate mannitol from the medium. Aliquots of mitochondrial samples were treated with 1 ml of 0.1 N sodium dodecyl sulphate, 1 ml of 0.1 HCL, 0.15 ml of 10% phosphotungstic acid, and 0.5 ml of 0.7% of 2-thiobarbituric acid. Butylated hydroxytoluene was added to a final concentration of 0.1% (w/v). The mixture was heated in boiling water for 60 min. TBARS were extracted in 5 ml of n-butanol. After a brief centrifugation, the fluorescence of the butanolic layer was measured at 515 nm (excitation) and 553 nm (emission). The values were expressed as nmol of TBARS per milligram of protein, using a malondialdehyde standard prepared from 1,1,3,3-tetramethoxypropane.

Superoxide dismutase activity

Superoxide dismutase activity was determined in cortical and striatal mitochondrial samples (0.25–0.75 mg protein/ml) by measuring the inhibition of autocatalytic adrenochrome formation rate in a reaction medium containing 1 mM epinephrine and 50 mM glycine-NaOH (pH 10.2). Enzyme activity was expressed as U_{SOD}/mg protein [25].

Aconitase and fumarase activities

Aconitase and fumarase activities were measured in cortical and striatal mitochondrial samples from control and paraquat-treated animals using spectrophotometric rate determination [26]. Freshly isolated mitochondria samples were sonicated (4 bursts of 30 s ON and 60 s OFF) followed by centrifugation at 8250 *g* for 10 min at 4°C. Specific activity of the mitochondrial aconitase present in the supernatant was measured by monitoring the conversion of sodium citrate to α-ketoglutarate at 25°C at 340 nm ($\varepsilon = 6.13$ mM^{-1} cm^{-1}) using the coupled reduction of $NADP^+$ to NADPH by isocitrate dehydrogenase. The reaction medium contains 50 mM Tris-HCl buffer (pH 7.4), 0.6 mM $MnCl_2$, 5 mM sodium citrate, 0.2 mM $NADP^+$, 0.25 mg mitochondrial protein/ml, and 1 U/ml isocitrate dehydrogenase. One milliunit of aconitase activity was defined as the amount of enzyme that catalyzes the formation of 1 nmol of isocitrate/minute [26]. The specific activity of fumarase was subsequently determined by following spectrophotometrically the conversion of malate to fumarate at 240 nm in a reaction medium containing 50 mM phosphate buffer (pH 7.4), 0.25 mg mitochondrial protein/ml, and 0.05 M sodium L-malate at 25°C. The ratio of the specific activities of aconitase to fumarase was then calculated. Aconitase reactivation was achieved by incubation of mitochondrial samples at different times with reducing reagents, 2 mM dithiothreitol and 0.2 mM ferrous ammonium sulphate. Then, the enzyme activity assay was repeated as described above.

Immunoblotting

Cortical and striatal mitochondrial and cytosolic fractions from control and paraquat-treated animals were prepared in Laemmli buffer with 2-mercaptoethanol (1:2 v/v) and boiled for 1 min. Equal amounts of protein (80 μg) were loaded onto SDS-PAGE (7.5% or 15%), separated and blotted onto nitrocellulose membranes in Tris-glycine-MeOH buffer. Non-specific binding was blocked by incubation of the membranes with 5% non-fat dry milk in PBS for 1 h at room temperature. The blots were probed with a dilution 1:500 of primary antibodies specific for Bax (amino terminus, N-20), Bcl-xl (amino terminus, S-18), Bak (G-23), cytochrome *c* (carboxi terminus, C-20), AIF (carboxi terminus, D-20), β-actin (C4), or cytochrome oxidase subunit III (MS406). Primary antibodies were incubated in 1% BSA in PBS overnight at 4°C with rocking. The blots were rinsed thrice for 15 min with PBST (PBS with 0.15% Tween 20) and then incubated with horseradish peroxidase-conjugated secondary antibodies (anti-mouse, anti-rabbit, anti-goat) at 1:5000 in 2.5% non-fat dry milk in PBS for 1 h at room temperature with rocking. The blots were rinsed thrice for 10 min with PBS and then exposed with ECL reagent [27,28]. Densitometric analysis of bands was performed using the NIH Image 1.54 software. All experiments were performed in triplicate.

Materials

Paraquat (1,1′-dimethyl-4,4′-bipyridinium dichloride), 2-thiobarbituric acid, EDTA, glutamic acid, isocitrate dehydrogenase, malic acid, mannitol, $MnCl_2$, $NADP^+$, phosphotungstic acid, sodium citrate, succinate, sucrose, Trizma base, and antimycin were purchased from Sigma Chemical Co (St. Louis, MO, USA). Other reagents were of analytical grade. MitoSOX and NAO were purchased

from Molecular Probes. Primary and secondary antibodies were provided by Santa Cruz Biotechnology Inc, USA. Cytochrome oxidase subunit III antibody was provided by MitoSciences Inc, USA.

Statistical analysis

Results were presented as mean ± SEM. Prior to each analysis, test variables were checked for normality so all data were evaluated by the Kolmogorov–Smirnov test. ANOVA followed by Tukey's test was used to analyze differences between mean values of more than two groups. SPSS (13.0 version) statistical software was used and a difference was considered to be statistically significant when $p < 0.05$.

Results

Paraquat increases cortical and striatal MitoSOX fluorescence

Mitochondria were loaded with MitoSOX, a fluorescent dye that typically increases its emission in the presence of an excessive generation of superoxide anion escaping from the action of Mn-SOD.

Typical experiments showing FL-2 histograms corresponding to cortical and striatal mitochondria are shown in Figure 1A and B, respectively. Basal MitoSox fluorescence was higher in striatal (A-i) than in cortical mitochondria (B-i). Cortical and striatal mitochondria from paraquat-treated animals showed an increased FL-2 fluorescence as compared with control mitochondria. Quantification of the superoxide anion levels was performed as the MitoSOX r.f.i. using marker 1 (M1), as shown in Figure 1C. M1 indicates high r.f.i. of the mitochondrial population. Striatal mitochondrial superoxide anion levels were significantly higher (42%) than in cortical mitochondria from untreated animals. Paraquat treatment increased cortical and striatal mitochondrial superoxide anion levels by 45% and 18%, respectively, as compared with control mitochondria. As expected, cortical and striatal mitochondria from control animals exposed to 0.5 μM antimycin showed an increased FL-2 fluorescence as compared with the basal values (positive control). Unloaded (no probe) mitochondrial sample was illustrated at the inset.

Paraquat increases cortical and striatal lipid peroxidation levels

TBARS production was 25% significantly higher in striatal mitochondria than in cortical mitochondria from untreated animals. Paraquat treatment increased cortical and striatal lipid peroxidation levels by 16% and 28%, respectively, as compared with control mitochondria (Figure 2).

Paraquat decreases cardiolipin content in cortical and striatal mitochondria

Previous observations indicate that low NAO fluorescence would be due to oxidation/depletion of cardiolipin [23,29,30]. This can be explained by the fact that free radicals-induced cardiolipin damage leads to a decreased cardiolipin accessibility to NAO.

Cortical and striatal mitochondria were analyzed for NAO staining by flow cytometry (Figure 3A and B). Unloaded (no probe) mitochondrial sample was illustrated at the insets. After NAO mitochondrial loading, we

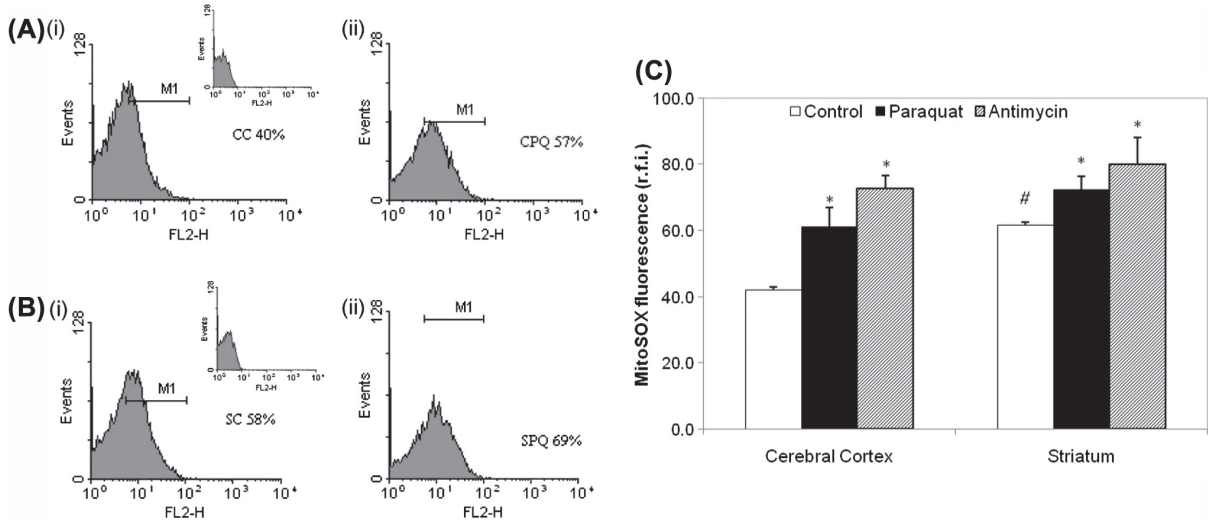

Figure 1. *Effects of paraquat treatment on cortical MitoSOX fluorescence intensity.* Histograms of cortical (A) and striatal (B) mitochondrial events versus r.f.i. (FL-2) from control (i) and paraquat-treated animals (ii). Samples without probe were used for autofluorescence (insets). CC: cerebral cortex from control animals, CPQ: cerebral cortex from paraquat-treated animals. SC: striatum from control animals and SPQ: striatum from paraquat-treated animals. Each histogram represents a typical experiment out of three. (C) A common marker (M1), indicating high relative fluorescence intensity of the mitochondrial population was used to quantify the superoxide anion levels in each experiment. Bars graph for quantification of mitochondrial MitoSOX relative fluorescence values (r.f.i.) as mitochondrial superoxide levels. Bars represent the mean ± SEM of three different experiments. Antimycin A was used as positive control. ANOVA followed by Tukey's test was used ($^{\#}p < 0.01$ as compared with cortical control value; $^{*}p < 0.01$, as compared with its respective control value).

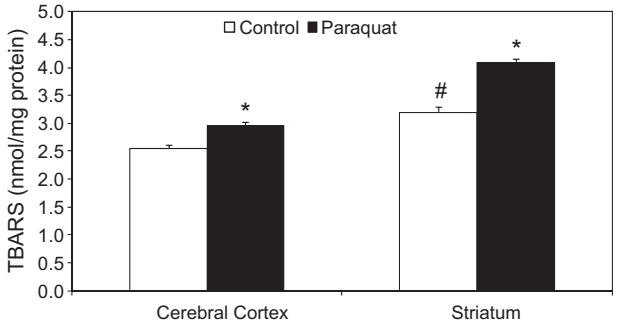

Figure 2. *Effect of paraquat on TBARS production*. Bars represent the mean ± SEM of three individual mitochondrial samples, each obtained from a pool of cerebral cortex or striatum of three rats. ANOVA followed by Tukey's test was used ($^{\#}p < 0.01$ as compared with cortical control value; $^{*}p < 0.001$, as compared with its respective control value).

quantified the amount of events with high fluorescence (M1) present in mitochondria from control and paraquat-treated animals in order to carefully evaluate the FL-2 fluorescence changes in the different samples. M1 describes a mitochondrial population with high cardiolipin content. Quantification of NAO r.f.i. under M1 was presented in Figure 3C. Striatal mitochondria from untreated animals presented 32% lower cardiolipin content than cortical mitochondria. Paraquat treatment decreased cortical and striatal NAO relative fluorescence by 13% and 49%, respectively ($p < 0.01$, as compared with control mitochondria), indicating cardiolipin peroxidation. Antimycin A (0.5 μM), an inhibitor of the ubiquinone-cytochrome *c* reductase, was used as a positive control.

Paraquat treatment increases cortical and striatal Mn-SOD activity

Increases of 73% and 79% were observed in Mn-SOD activity in cortical and striatal mitochondrial samples, respectively, after paraquat treatment ($p < 0.05$, as compared with control values) (Figure 4).

Paraquat treatment decreases cortical and striatal mitochondrial aconitase activity

Mitochondrial aconitase activity is a functional indicator of mitochondrial levels of reactive oxygen species because its iron-sulfur core is frequently oxidized by superoxide anion, reducing the enzyme activity. However, mitochondrial reactive oxygen species do not affect fumarase activity. Therefore, we used the activity ratio between mitochondrial aconitase and fumarase as a functional indicator of the presence of oxidative stress. As shown in Figure 5, striatal mitochondria presented a 45% lower aconitase/fumarase activity ratio than cortical mitochondria in untreated animals. The ratios of mitochondrial aconitase to fumarase activity were significantly decreased by 41% and 53% in cerebral cortex and striatum, respectively, after paraquat treatment ($p < 0.01$, as compared with control values). Exposure

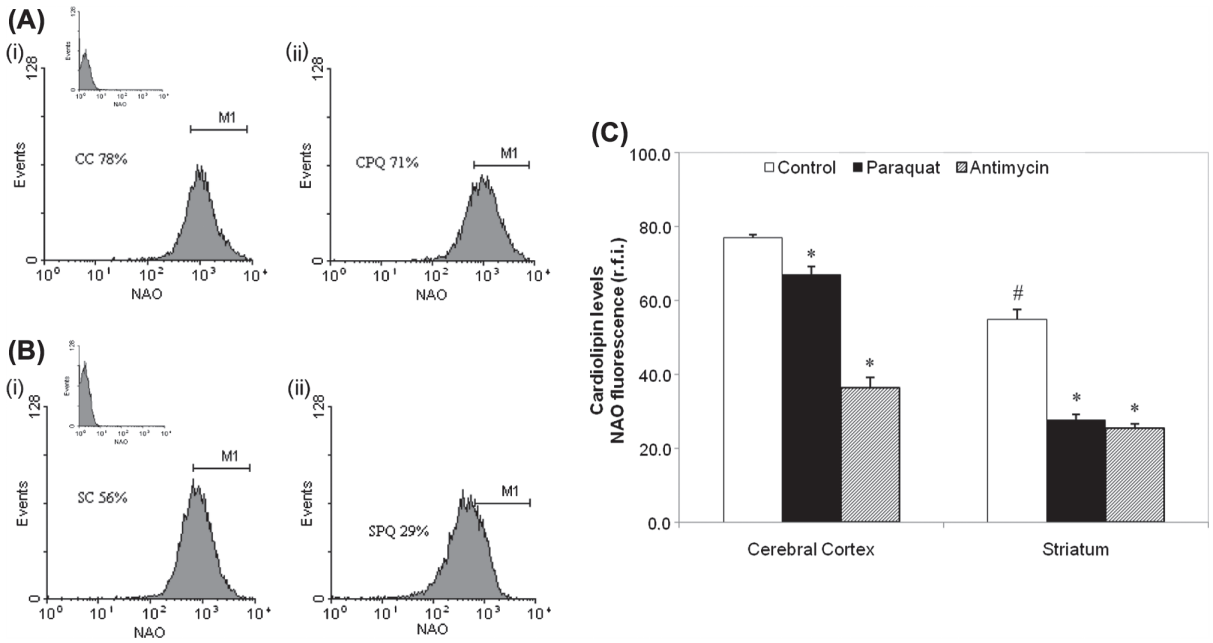

Figure 3. *Effects of paraquat treatment on NAO fluorescence*. Histograms of cortical (A) and striatal (B) mitochondrial events versus r.f.i. (FL-2) from control (i) and paraquat-treated animals (ii). Autofluorescence was evaluated without probe (insets). CC: cerebral cortex from control animals, CPQ: cerebral cortex from paraquat-treated animals. SC: striatum from control animals and SPQ: striatum from paraquat-treated animals. Each histogram represents a typical experiment out of three. (C) Bars graph quantification of the amount of events with high NAO relative fluorescence was conducted using a marker (M1), indicative of the level of cardiolipin content. Bars represent the mean ± SEM of three different experiments. Antimycin A was used as positive control of lipid peroxidation. ANOVA followed by Tukey's test was used ($^{\#}p < 0.05$ as compared with cortical control value; $^{*}p < 0.01$, as compared with its respective control value).

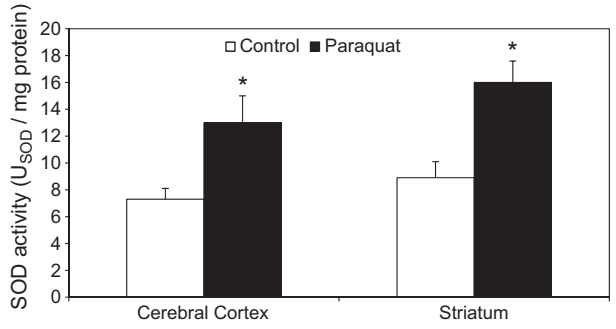

Figure 4. *Effect of paraquat treatment on Mn-SOD activity.* Bars represent $U_{SOD} \pm$ SEM of three individual mitochondrial samples, each obtained from a pool of cerebral cortex or striatum of three rats. ANOVA followed by Tukey's test was used (*$p < 0.05$ as compared with its respective control value).

of cortical and striatal mitochondrial samples from paraquat-treated animals to reducing agents during 1 h did not induce the reactivation of aconitase activity (data not shown).

Paraquat increases Bax and Bak expressions associated to mitochondrial membranes

An increased Bax association to the outer mitochondrial membrane was clearly observed after paraquat treatment in cerebral cortex and striatum as compared with control mitochondria (Figure 6A-i). Also, paraquat treatment increased Bak expression in cortical and striatal mitochondrial membranes (Figure 6B-i). However, Bcl-xl protein levels showed no differences after paraquat treatment in the studied brain areas (Figure 6A-i and B-i). Furthermore, Bax/Bcl-xl and Bak/Bcl-xl ratios were measured by band quantification. Paraquat treatment significantly increased Bax/Bcl-xl ratios by 1.5- and 1.2-fold and Bak/Bcl-xl ratios by 1.2- and 1-fold in cortical and striatal mitochondria, respectively ($p < 0.05$, as compared with control values) (Figure 6A-ii and B-ii).

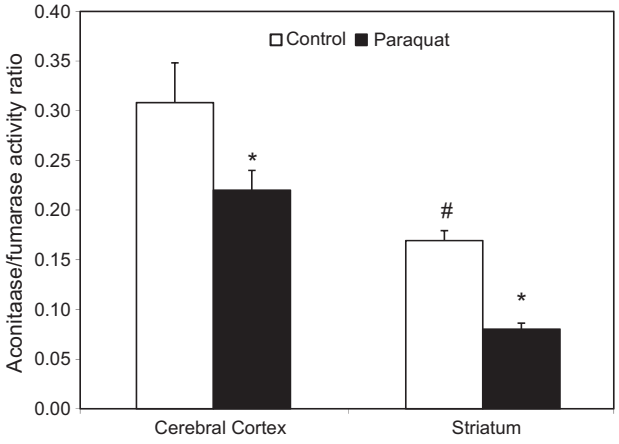

Figure 5. *Effect of paraquat treatment on aconitase activity.* Bars represent the aconitase/fumarase activity ratio ± SEM of four individual mitochondrial samples, each obtained from a pool of cerebral cortex or striatum of three rats. ANOVA followed by Tukey's test was used ($^{\#}p < 0.01$ as compared with cortical control value; *$p < 0.05$, as compared with its respective control value).

Paraquat induces cytochrome c and AIF release from mitochondria

Cytochrome *c* immunoreactivity was evident as a single band of 12 kDa in both subcellular fractions (Figure 7A). The ratios between the levels of cytochrome *c* observed in the mitochondrial pellet and in the cytosolic fractions clearly decreased by 93% and 89% after paraquat treatment in cortical and striatal samples, respectively ($p < 0.01$, as compared with control values) (Figure 7B). Also, paraquat treatment induced the release of AIF (57 kDa) into cytosol in both brain areas (Figure 8A). Significant decreases in AIF pellet/cytosol ratios of 96% and 93% were observed in cortical and striatal samples from paraquat-treated animals ($p < 0.01$, as compared with control values) (Figure 8B).

Discussion

This study was aimed at understanding the molecular mechanism involved in mitochondrial dysfunction and apoptosis in the premotor stages of Parkinson's disease. The results showed that *in vivo* paraquat treatment increases cortical and striatal intramitochondrial superoxide anion levels inducing a condition of oxidative stress, even in the presence of an increased Mn-SOD activity. The increased superoxide anion levels observed could be due to a permanent protein alteration of Complex I induced by paraquat as observed previously by our laboratory [15]. In this context, we evaluated the oxidative damage on aconitase activity. *In vitro* evidence indicates that aconitase is highly susceptible to prooxidant-induced inactivation, rather than a protein expression decrease [26,31]. Our results showed that chronic paraquat treatment inhibited aconitase activity in mitochondria from cerebral cortex and striatum. These results are in agreement with Bulteau et al. [32] that reported an irreversible aconitase inhibition by an increased or prolonged oxidative stress. We observed no reactivation of the enzyme after 1 h even in the presence of citrate as a substrate, indicating that aconitase inhibition was irreversible, probably due to the persistent inhibition of Complex I, which in turn induced high levels of superoxide.

Lipid peroxidation of mitochondrial membrane phospholipids is considered one of the major causes of mitochondrial dysfunction in a variety of pathophysiological situations [33,34]. Cardiolipin, a phospholipid of the inner mitochondrial membrane, is involved in several bioenergetics processes optimizing the activity of key mitochondrial inner proteins involved in oxidative phosphorylation [35]. The current study shows that increased intramitochondrial superoxide anion levels and the persistent inhibition of mitochondrial aconitase were associated with increased lipid peroxidation and cardiolipin oxidation/depletion in cerebral and striatal intact mitochondria, measured as TBARS production and NAO staining, respectively.

Important to note is the fact that the specificity of MitoSOX red (Mito-HE) for superoxide *in vivo* is limited by autooxidation as well as by nonsuperoxide-dependent

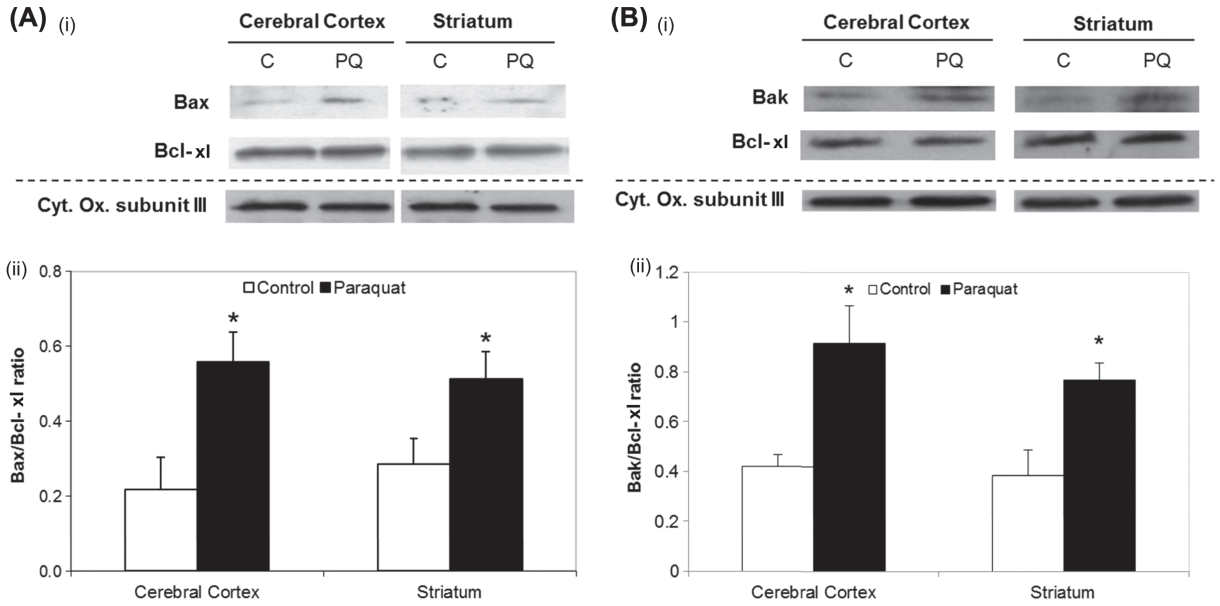

Figure 6. *Effects of paraquat treatment on mitochondrial Bax, Bak, and Bcl-xl protein expressions*.(A) *Bax -Bcl-xl* and (B) *Bak - Bcl-xl expression*. Typical examples of Western blots of mitochondrial samples of each experimental group (i). Cytochrome oxidase subunit III was used as loading control of mitochondrial fractions. C: control animals. PQ: paraquat-treated animals. The results are representative of three independent studies. (ii) Bars represent mitochondrial Bax/Bcl-xl or Bak/Bcl-xl ratio ± SEM obtained after densitometric analysis. ANOVA followed by Tukey's test was used (*$p < 0.05$, as compared with its respective control value).

processes that can oxidize HE probes [36]. Thus, in our study the results of increased MitoSOX superoxide detection were supported by the decreased aconitase activity and high cardiolipin peroxidation after paraquat treatment.

In addition, cortical and striatal mitochondria from untreated animals showed significantly different basal levels of superoxide anion and cardiolipin content as well as aconitase activity, as observed in Figures 1–4. These

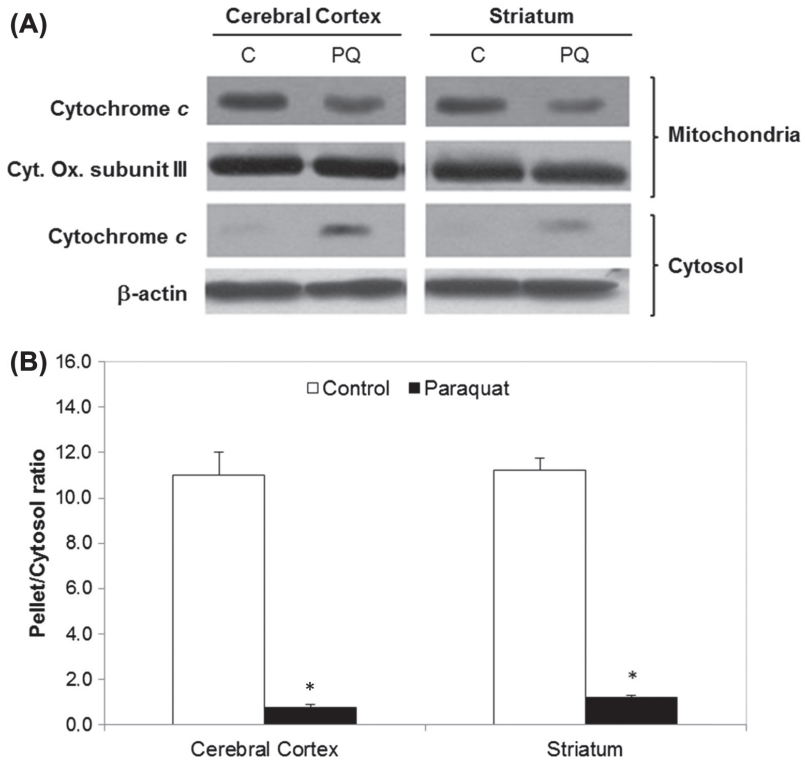

Figure 7. *Effects of paraquat treatment on cytochrome c release*. (A) Typical examples of Western blots of mitochondrial and cytosolic samples for each experimental group. Cytochrome oxidase subunit III and β-actin were used as loading control for mitochondrial and cytosolic fractions, respectively. C: control animals. PQ: paraquat treated animals. The results are representative of three independent studies. (B) Bars represent cytochrome *c* mitochondrial/cytosol ratio ± SEM obtained after densitometric analysis. ANOVA followed by Tukey's test was used (*$p < 0.01$, as compared with its respective control value).

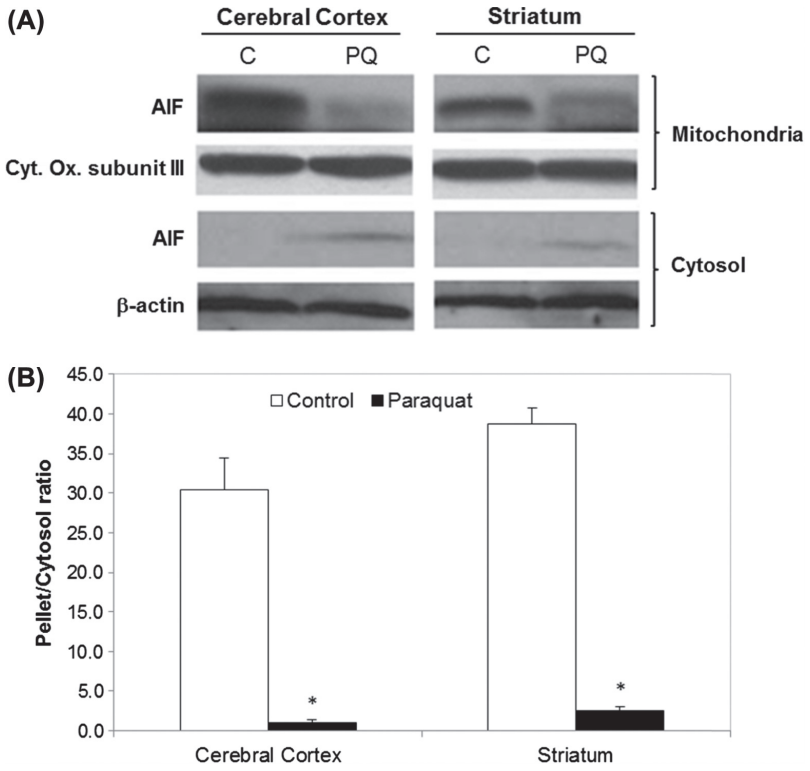

Figure 8. *Effects of paraquat treatment on AIF release*. (A) Typical examples of Western blots for mitochondrial and cytosolic samples for each experimental group. Cytochrome oxidase subunit III and β-actin were used as loading control of mitochondrial and cytosolic fractions, respectively. C: control animals. PQ: paraquat treated animals. The results are representative of three independent studies. (B) Bars represent AIF mitochondrial/cytosol ratio ± SEM obtained after densitometric analysis. ANOVA followed by Tukey's test was used (*$p < 0.01$, as compared with its respective control value).

differences could be attributed to the high oxidative dopamine metabolism present in the striatum [37]. In accordance, cardiolipin peroxidative damage and aconitase activity decrease were more marked in striatal mitochondria than in cerebral cortex after paraquat treatment. Data shown in this study could indicate that the endogenous oxidative metabolism present in striatal mitochondria turned this tissue more sensitive to chronic paraquat treatment. This result could be supported by Pickrell et al. [38] who observed that striatum is highly susceptible to mitochondrial oxidative phosphorylation dysfunctions.

Mitochondrial participation in paraquat-induced apoptosis was associated with the increased superoxide anion levels, high aconitase inactivation, and marked cardiolipin peroxidation leading to cortex and striatal activation of cell death pathways. It is well known that pro-apoptotic members of the Bcl-2 family are responsible for transient membrane permeabilization facilitating cytochrome *c* release [39]. In this study, paraquat induced the association of the pro-apoptotic protein Bax to cortical and striatal mitochondrial membranes. This association could be due to alterations in Complex I activity and subsequent increase in intramitochondrial superoxide anion levels, in accordance with previous studies showing that Complex I deficiency primes Bax-dependent neuronal apoptosis through mitochondrial oxidative stress [40]. Fei et al. [41] reported that paraquat triggers apoptosis in SK-N-SH cells through a Bak-dependent mitochondrial membrane depolarization, cytochrome *c* release, and caspase 3 activation. In contrast, our results suggest that in our model of paraquat neurotoxicity, Bax and Bak play an important role in mitochondrial membrane permeabilization.

It is known that impaired mitochondrial respiration linked to Complex I blockade leads to oxidative damage to proteins, lipids, and DNA and activation of mitochondria-dependent apoptotic machinery by directly triggering the release of the apoptogenic molecules from the defective mitochondria [42,43]. Cytochrome *c* normally present at the inner mitochondrial membrane is closely attached to cardiolipin molecules [44]. As expected, we observed that paraquat treatment decreased the levels of cytochrome *c* in cortical and striatal mitochondria and simultaneously induced an increase of this molecule in the cytosol. Also, it has been suggested that after an apoptotic insult, AIF translocates from mitochondria to the cytosol were its reaches the nucleus interacting with cyclophilin A to become an active DNAse [45,46]. Our data showed that paraquat treatment induced AIF release from cortical and striatal mitochondria to the cytosol. Taking into account the data presented here, we suggest that cytochrome *c* and AIF release was induced by paraquat treatment as a consequence of outer membrane permeabilization and cardiolipin peroxidation.

Although the striatum was more susceptible of undergoing oxidative damage than the cerebral cortex, similar levels of apoptosis were induced in both brain areas. We cannot discard that other types of cell demise could be occurring in the striatum characterized by different hybrids shapes between apoptosis and necrosis.

Conclusions

Differences in basal superoxide anion levels, cardiolipin content, and aconitase activity were observed in cortical and striatal mitochondria from untreated animals, probably due to a high oxidative metabolic state present in striatal tissue. In addition a weekly dose of paraquat (10 mg/kg *ip*) during four weeks activates intrinsic mitochondrial pathways associated with cell death program such as the induction of Bak and Bax pathways on mitochondrial membranes, changes in permeability to the cardiolipin detached cytochrome *c* and the loss of the protein factor AIF from the inner membrane to the cytosol. Interesting to note was the fact that under chronic paraquat exposure, striatal mitochondria showed higher sensitivity to paraquat oxidative damage as compared with brain cortex mitochondria. Even in the presence of a higher oxidative stress in the striatum, the levels of proapoptotic proteins attained in the mitochondria were similar in both brain areas.

Acknowledgments

We thank to Dr Rodolfo Cutrera and Lic Analia Karadayian from the Laboratory of Neurobiology and Rhythms (School of Medicine, University of Buenos Aires, Argentina) for their collaboration during this research.

Declaration of interest

The authors report no conflict of interest. The authors alone are responsible for the content and writing of the paper.

This research was supported by grants from Universidad de Buenos Aires (B025 and 20020100100511) and Consejo Nacional de Investigaciones Científicas y Técnicas (PIP112-200801-00653), Argentina.

References

[1] McCormack AL, Thiruchelvam M, Manning-Bog AB, Thiffault C, Langston JW, Cory-Slechta DA, Di Monte DA. Environmental risk factors and Parkinson's disease: selective degeneration of nigral dopaminergic neurons caused by the herbicide paraquat. Neurobiol Dis 2002;10:119–127.

[2] Ossowska K, Wardas J, Smialowska M, Kuter K, Lenda T, Wieronska JM, et al. A slowly developing dysfunction of dopaminergic nigrostriatal neurons induced by long-term paraquat administration in rats: an animal model of preclinical stages of Parkinson's disease? Eur J Neurosci 2005;22:1294–1304.

[3] Shimizu K, Matsubara K, Ohtaki K, Fujimaru S, Saito O, Shiono H. Paraquat induces long-lasting dopamine overflow through the excitotoxic pathway in the striatum of freely moving rats. Brain Res 2003;976:243–252.

[4] Thiruchelvam M, Richfield EK, Baggs RB, Tank AW, Cory-Slechta DA. The nigrostriatal dopaminergic system as a preferential target of repeated exposures to combined paraquat and maneb: implications for Parkinson's disease. J Neurosci 2000;20:9207–9214.

[5] Prasad K, Tarasewicz E, Mathew J, Strickland PA, Buckley B, Richardson JR, Richfield EK. Toxicokinetics and toxicodynamics of paraquat accumulation in mouse brain. Exp Neurol 2009;215:358–367.

[6] Bove J, Prou D, Perier C, Przedborski S. Toxin-induced models of Parkinson's disease. NeuroRx 2005;2:484–494.

[7] Chen Q, Niu Y, Zhang R, Guo H, Gao Y, Li Y, Liu R. The toxic influence of paraquat on hippocampus of mice: involvement of oxidative stress. Neurotoxicology;31:310–316.

[8] Franco R, Li S, Rodriguez-Rocha H, Burns M, Panayiotidis MI. Molecular mechanisms of pesticide-induced neurotoxicity: Relevance to Parkinson's disease. Chem Biol Interact 2010;188:289–300.

[9] Litteljohn D, Nelson E, Bethune C, Hayley S. The effects of paraquat on regional brain neurotransmitter activity, hippocampal BDNF and behavioural function in female mice. Neurosci Lett 2011;502:186–191.

[10] Lin MT, Beal MF. Mitochondrial dysfunction and oxidative stress in neurodegenerative diseases. Nature 2006;443: 787–795.

[11] Schon EA, Manfredi G. Neuronal degeneration and mitochondrial dysfunction. J Clin Invest 2003;111:303–312.

[12] Cocheme HM, Murphy MP. Complex I is the major site of mitochondrial superoxide production by paraquat. J Biol Chem 2008;283:1786–1798.

[13] Fukushima T, Yamada K, Isobe A, Shiwaku K, Yamane Y. Mechanism of cytotoxicity of paraquat. I. NADH oxidation and paraquat radical formation via complex I. Exp Toxicol Pathol 1993;45:345–349.

[14] Tawara T, Fukushima T, Hojo N, Isobe A, Shiwaku K, Setogawa T, Yamane Y. Effects of paraquat on mitochondrial electron transport system and catecholamine contents in rat brain. Arch Toxicol 1996;70:585–589.

[15] Czerniczyniec A, Karadayian AG, Bustamante J, Cutrera RA, Lores-Arnaiz S. Paraquat induces behavioral changes and cortical and striatal mitochondrial dysfunction. Free Radic Biol Med 2011;51:1428–1436.

[16] Ossowska K, Smialowska M, Kuter K, Wieronska J, Zieba B, Wardas J, et al. Degeneration of dopaminergic mesocortical neurons and activation of compensatory processes induced by a long-term paraquat administration in rats: implications for Parkinson's disease. Neuroscience 2006;141:2155–2165.

[17] Madison DV, Edson EB. Preparation of hippocampal brain slices. Curr Protoc Neurosci 2001;Chapter 6:Unit 6 4.

[18] Lowry OH, Rosebrough NJ, Farr AL, Randall RJ. Protein measurement with the Folin phenol reagent. J Biol Chem 1951;193:265–275.

[19] Bustamante J, Di Libero E, Fernandez-Cobo M, Monti N, Cadenas E, Boveris A. Kinetic analysis of thapsigargin-induced thymocyte apoptosis. Free Radic Biol Med 2004;37: 1490–1498.

[20] McMillin JB, Dowhan W. Cardiolipin and apoptosis. Biochim Biophys Acta 2002;1585:97–107.

[21] Petit JM, Maftah A, Ratinaud MH, Julien R. 10N-nonyl acridine orange interacts with cardiolipin and allows the quantification of this phospholipid in isolated mitochondria. Eur J Biochem 1992;209:267–273.

[22] Wright MM, Howe AG, Zaremberg V. Cell membranes and apoptosis: role of cardiolipin, phosphatidylcholine, and anticancer lipid analogues. Biochem Cell Biol 2004;82:18–26.

[23] Nomura K, Imai H, Koumura T, Kobayashi T, Nakagawa Y. Mitochondrial phospholipid hydroperoxide glutathione peroxidase

inhibits the release of cytochrome c from mitochondria by suppressing the peroxidation of cardiolipin in hypoglycaemia-induced apoptosis. Biochem J 2000;351:183–193.
[24] Esterbauer H, Cheeseman KH, Dianzani MU, Poli G, Slater TF. Separation and characterization of the aldehydic products of lipid peroxidation stimulated by ADP-Fe2 + in rat liver microsomes. Biochem J 1982;208:129–140.
[25] Misra HP, Fridovich I. The role of superoxide anion in the autoxidation of epinephrine and a simple assay for superoxide dismutase. J Biol Chem 1972;247:3170–3175.
[26] Gardner PR. Aconitase: sensitive target and measure of superoxide. Methods Enzymol 2002;349:9–23.
[27] Boveris A, Arnaiz SL, Bustamante J, Alvarez S, Valdez L, Boveris AD, Navarro A. Pharmacological regulation of mitochondrial nitric oxide synthase. Methods Enzymol 2002;359: 328–39.
[28] Bustamante J, Bersier G, Badin RA, Cymeryng C, Parodi A, Boveris A. Sequential NO production by mitochondria and endoplasmic reticulum during induced apoptosis. Nitric Oxide 2002;6:333–341.
[29] Paradies G, Petrosillo G, Pistolese M, Ruggiero FM. The effect of reactive oxygen species generated from the mitochondrial electron transport chain on the cytochrome c oxidase activity and on the cardiolipin content in bovine heart submitochondrial particles. FEBS Lett 2000;466:323–326.
[30] Paradies G, Petrosillo G, Pistolese M, Ruggiero FM. Reactive oxygen species generated by the mitochondrial respiratory chain affect the complex III activity via cardiolipin peroxidation in beef-heart submitochondrial particles. Mitochondrion 2001;1:151–159.
[31] Cantu D, Fulton RE, Drechsel DA, Patel M. Mitochondrial aconitase knockdown attenuates paraquat-induced dopaminergic cell death via decreased cellular metabolism and release of iron and H(2)O(2). J Neurochem 2011;118:79–92.
[32] Bulteau AL, Ikeda-Saito M, Szweda LI. Redox-dependent modulation of aconitase activity in intact mitochondria. Biochemistry 2003;42:14846–14855.
[33] Pamplona R. Membrane phospholipids, lipoxidative damage and molecular integrity: a causal role in aging and longevity. Biochim Biophys Acta 2008;1777:1249–1262.
[34] Paradies G, Petrosillo G, Paradies V, Ruggiero FM. Role of cardiolipin peroxidation and Ca2 + in mitochondrial dysfunction and disease. Cell Calcium 2009;45:643–650.
[35] Petrosillo G, Portincasa P, Grattagliano I, Casanova G, Matera M, Ruggiero FM, et al. Mitochondrial dysfunction in rat with nonalcoholic fatty liver Involvement of complex I, reactive oxygen species and cardiolipin. Biochim Biophys Acta 2007;1767:1260–1267.
[36] Robinson KM, Janes MS, Pehar M, Monette JS, Ross MF, Hagen TM, Murphy MP, Beckman JS. Selective fluorescent imaging of superoxide in vivo using ethidium-based probes. Proc Natl Acad Sci U S A 2006;103:15038–43.
[37] Lai CT, Yu PH. Dopamine- and L-beta-3,4-dihydroxyphenylalanine hydrochloride (L-Dopa)-induced cytotoxicity towards catecholaminergic neuroblastoma SH-SY5Y cells. Effects of oxidative stress and antioxidative factors. Biochem Pharmacol 1997;53:363–372.
[38] Pickrell AM, Fukui H, Wang X, Pinto M, Moraes CT. The striatum is highly susceptible to mitochondrial oxidative phosphorylation dysfunctions. J Neurosci 2011;31: 9895–9904.
[39] Green DR. Life, death, BH3 profiles, and the salmon mousse. Cancer Cell 2007;12:97–99.
[40] Perier C, Tieu K, Guegan C, Caspersen C, Jackson-Lewis V, Carelli V, et al. Complex I deficiency primes Bax-dependent neuronal apoptosis through mitochondrial oxidative damage. Proc Natl Acad Sci U S A 2005;102:19126–19131.
[41] Fei Q, McCormack AL, Di Monte DA, Ethell DW. Paraquat neurotoxicity is mediated by a Bak-dependent mechanism. J Biol Chem 2008;283:3357–3364.
[42] Clayton R, Clark JB, Sharpe M. Cytochrome c release from rat brain mitochondria is proportional to the mitochondrial functional deficit: implications for apoptosis and neurodegenerative disease. J Neurochem 2005;92:840–849.
[43] Green DR, Kroemer G. The pathophysiology of mitochondrial cell death. Science 2004;305:626–629.
[44] Rytomaa M, Mustonen P, Kinnunen PK. Reversible, nonionic, and pH-dependent association of cytochrome c with cardiolipin-phosphatidylcholine liposomes. J Biol Chem 1992;267: 22243–22248.
[45] Daugas E, Susin SA, Zamzami N, Ferri KF, Irinopoulou T, Larochette N, et al. Mitochondrio-nuclear translocation of AIF in apoptosis and necrosis. Faseb J 2000;14:729–739.
[46] Cande C, Vahsen N, Kouranti I, Schmitt E, Daugas E, Spahr C, et al. AIF and cyclophilin A cooperate in apoptosis-associated chromatinolysis. Oncogene 2004;23:1514–1521.